Electronic Supplementary Information (ESI)

Penetrated 2D/3D Hybrid Heterojunction for High-Performance Perovskite Solar Cells

Jianguo Sun[a], Xuliang Zhang[a], Xufeng Ling[a], Yingguo Yang[b], Yao Wang[a], Junjun Guo[a], Shengzhong (Frank) Liu[c], Jianyu Yuan[a,]*and Wanli Ma[a,]*

[a]Institute of Functional Nano & Soft Materials (FUNSOM), Jiangsu Key Laboratory for Carbon-Based Functional Materials & Devices, Soochow University, 199 Ren-Ai Road, Suzhou Industrial Park, Suzhou, Jiangsu 215123, P. R. China Email: jyyuan@suda.edu.cn, wlma@suda.edu.cn

[b]Shanghai Synchrotron Radiation Facility, Shanghai Institute of Applied Physics, Chinese Academy of Sciences, Shanghai 201204, P. R. China.

[c]Shaanxi Normal University, Key Laboratory of Applied Surface and Colloid Chemistry, MOE, School of Materials Science and Engineering, Xi'an, CN 710062.

1. Materials

Lead iodide (PbI_2) and cesium iodide (CsI) were purchased from Alfa Aesar. Lead bromide ($PbBr_2$), formamidinium iodide (FAI), methylammonium bromide (MABr), DMAI, and 4-tert-butylpyridine (tBP) were purchased from Xi'an Polymer Light Technology. Spiro-OMeTAD was purchased from Advanced Election Technology Co., Ltd. Bis(trifluoromethylsulfonyl)imide lithium salt (Li-TFSI), acetonitrile (ACN), IPA, dimethylformamide (DMF), dimethyl sulfoxide (DMSO) and chlorobenzene (CB) were purchased from Sigma Aldrich. All the chemicals were used as received without further purification.

2. Solution preparation

Perovskite precursor solution was prepared by dissolving 1.3 M PbI_2, 1.2 M FAI, 0.14 M $PbBr_2$, 0.14 M MABr and 0.07 M CsI in a mixed solvent of DMF and DMSO (volume ratio 8:2). Solution for post treatment was realized by dissolving DMAI in IPA at various concentrations. The 90 mg of Spiro-OMeTAD was dissolved in 1 mL of chlorobenzene with 35.5 µL of t-BP and 20.63 µL of Li-TFSI (520 mg mL^{-1} in ACN) for hole transporting layer fabrication.

3. Device Fabrication and Characterization

The compact TiO2 film with 40 nm thickness was deposited onto the cleaned FTO substrates by chemical bath deposition.48 Before depositing the perovskite film, the TiO2 substrates were annealed at 200 °C for 30 min and then exposed to UV-ozone for 15 min. 30 µL of perovskite precursor solution was spin coated on the compact TiO_2 with a two steps procedure at 1000 rpm with an acceleration of 200 rpm/s for 10 s and 6000 rpm with an acceleration of 2000 rpm/s for 20 s in a nitrogen glove box. 180 µL of CB was dropped on the spinning substrate at 8 s before the second procedure finishes and the film were subsequently

annealed on a hotplate at 100 °C for 1 h. For constructing a 2D/3D heterojunction, 100 µL of DMAI/IPA solution was spin coated on the 3D perovskite surface at 5000 rpm with an acceleration of 2000 rpm/s for 30 s, and annealed at 100 °C for 5 min. After the substrates cooled down to room temperature, 30 µL of Spiro-OMeTAD was spin-coated on the perovskite layers at 4000 rpm with an acceleration of 2000 rpm/s for 20 s. Finally, 8 nm of MoO3 and 120 nm of Ag electrodes were subsequently deposited by thermal evaporation under a vacuum of 2×10-6 mbar to complete the whole device fabrication. For stability characterization, the MoO3 and Ag were replaced by 80 nm of Au. The single device has an active area of 7.25 mm−2. The current density-voltage (J-V) characteristics of the devices were obtained through a Keithley 2400 digital source meter under simulated AM 1.5G spectrum at 100 mW cm−2 in ambient air conditions with a solar simulator (Class AAA, 94023A-U, Newport). The devices were measured with a scan rate of 100 mV/s. The EQE spectra of the cells were tested through a certified incident photo-to-electron conversion efficiency equipment (Solar Cell Scan 100, Zolix Instruments Co. Ltd.).

4. Characterizations

UV-vis spectra were recorded on a PerkinElmer model Lambda 750. The steady-state and time-resolved PL spectra were recorded with a FluoroMax-4 spectrofluorometer (HORIBA Scientific). GIWAXS measurements were performed at the Shanghai Synchrotron Radiation Facility Laboratory on Beamline BL14B1 using X-rays with a wavelength of λ= ~1.24 Å. The XPS spectra were obtained using a Kratos AXIS Ultra DLD ultrahigh vacuum photoemission spectroscopy system, with an Al Ka radiation source. UPS measurements were performed using an Omicron Nanotechnology system with a base pressure of 2×10^{-10} Torr. Top-view and cross-section SEM images were characterized by a Zeiss Supra 55 field in high vacuum mode

at 15 kV accelerating voltage. AFM images (tapping mode) were captured through an Asylum Research Cypher S AFM microscope. Conductive-AFM (Veeco Metrology) was used to detect the conductivity and carrier transport properties of the film under the bias applied reverse to the FTO substrate under low intensity light illumination provided by AFM setup in a N_2 grove box. TOF-SIMS (GAIA3 GMU Model 2016/*GAIA3) was used for elemental analysis and mapping. ITO/3D Perovskite/2D Perovskite structure was adopted to fulfill this measurement. EIS measurements were carried out through Zahner IM6 electrochemical workstation while applying a bias of under open-circuit with a frequency between 0.25 MHz and 0.05 Hz under a monochromatic LED (500 nm, 100 mW) light irradiation.

5. SCLC measurements

Structure of FTO/TiO_2/Perovskite/PCBM/Ag and ITO/PEDOT:PSS/Perovskite/Spiro-OMeTAD/Ag were applied for electron-only and hole-only devices, respectively. The trap-state density (n_t) of the perovskite film can be calculated by the equation:

$$n_t = \frac{2\varepsilon_0\varepsilon_r V_{TFL}}{qL^2}$$

Where ε_0 is the vacuum permittivity, ε_r is the relative permittivity, V_{TFL} is trap-filled limit voltage, q is the elementary charge, and L is the thickness of perovskite film.

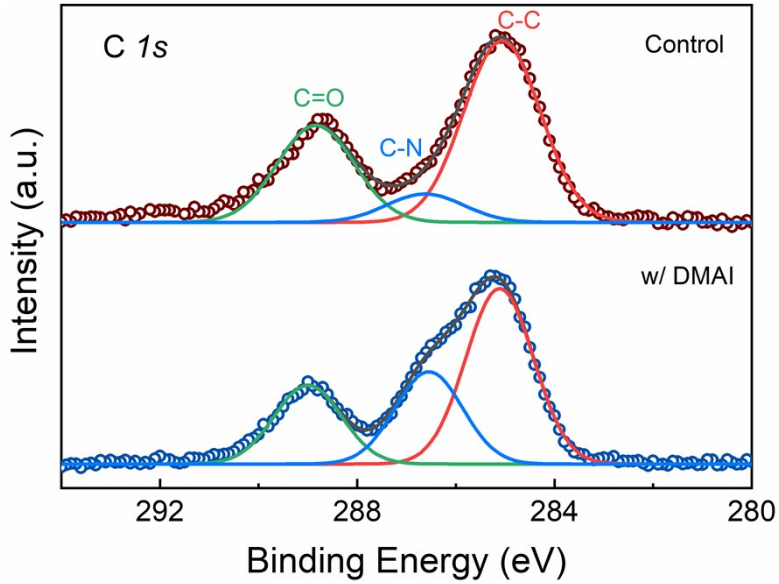

Fig. S1 The XPS core level spectra of C *1s*. It should be noted that the decreased intensity of C=O can be attributed to the hydrophobic nature of DMA^+.

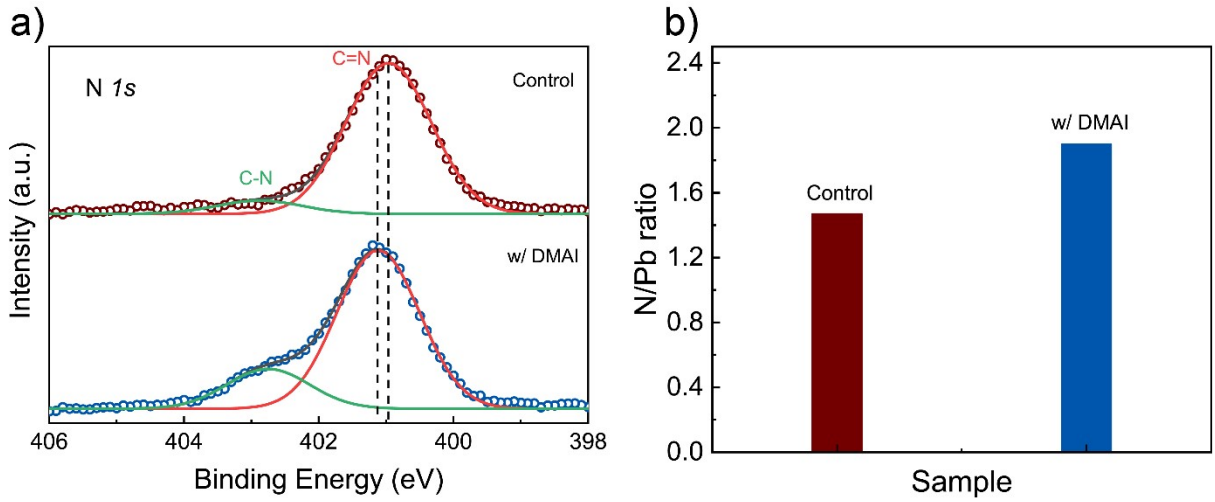

Fig. S2 a) The XPS core level spectra of N *1s*. The peak at ~401 eV binding energy is attributed to the C=N bonds of the FA cation, and the peak at ~402.5 eV that comes from the C–N bonds of the MA cation in the control perovskite film, the shifted C=N showed that chemical

environment of FA had changed. b) Statistical N/Pb atomic ratio, a clear increase in the N/Pb ratio indicated that the DMAI had been successfully introduced.

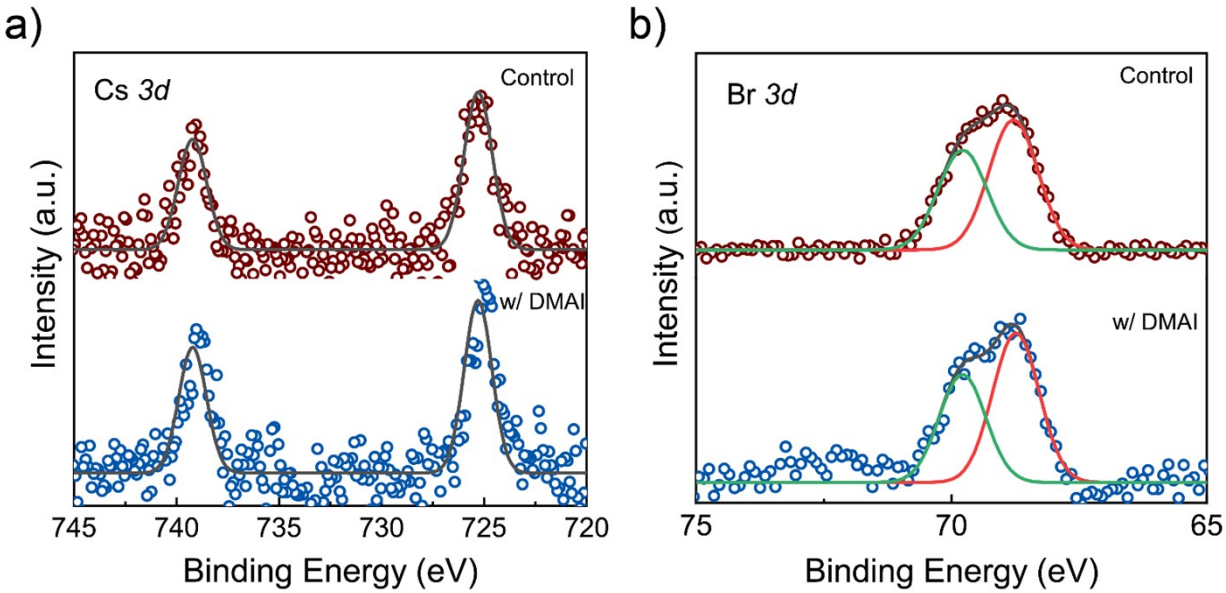

Fig. S3 The XPS core level spectra of a) Cs *3d* and b) Br *3d*, which both shows the negligible shift.

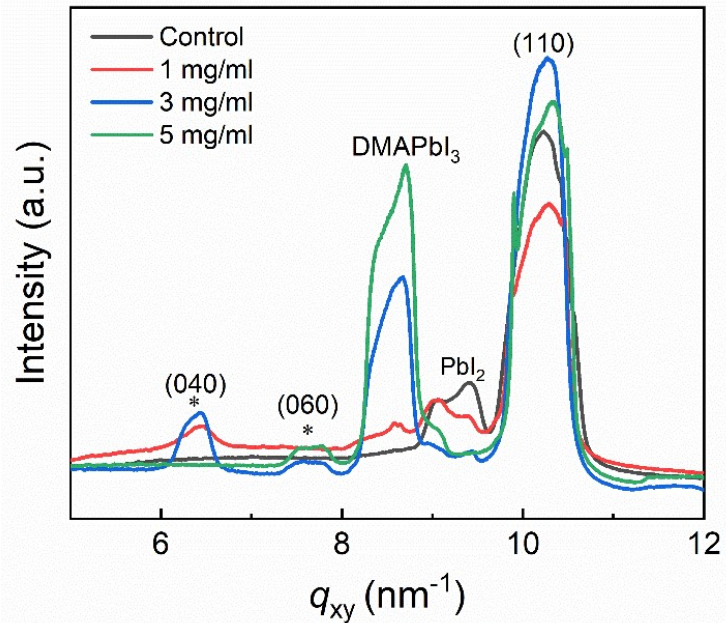

Fig. S4 Intensity profiles along the out-of-plane direction of the 2D GIWAXS patterns. A peak located at 6.42 nm and 7.64 are the typical (040) and (060) plane of 2D perovskite for 1 mg mL^{-1} and 3 mg mL^{-1} (our optimal concentration) DMAI treated perovskite film, respectively.

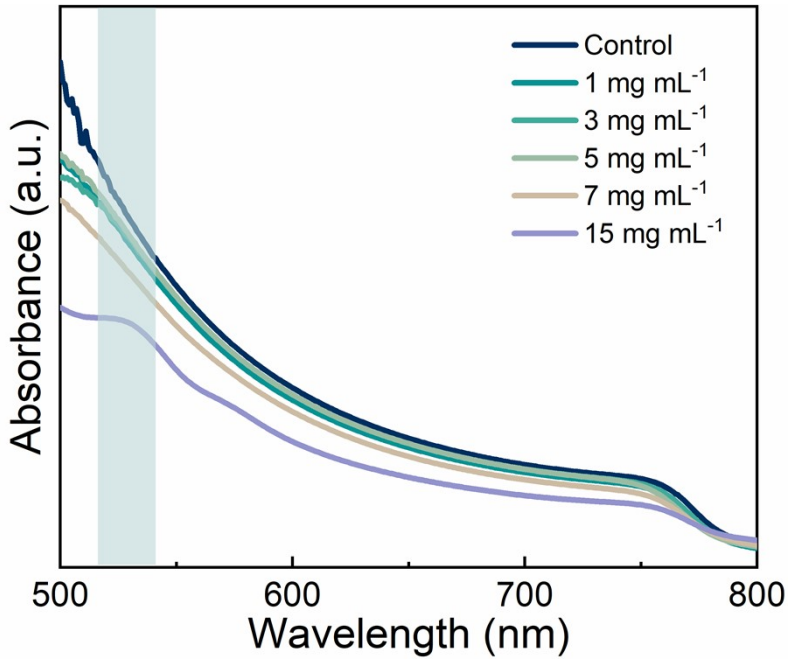

Fig. S5 UV-vis absorption spectrum of perovskite film treated by different concentration of DMAI.

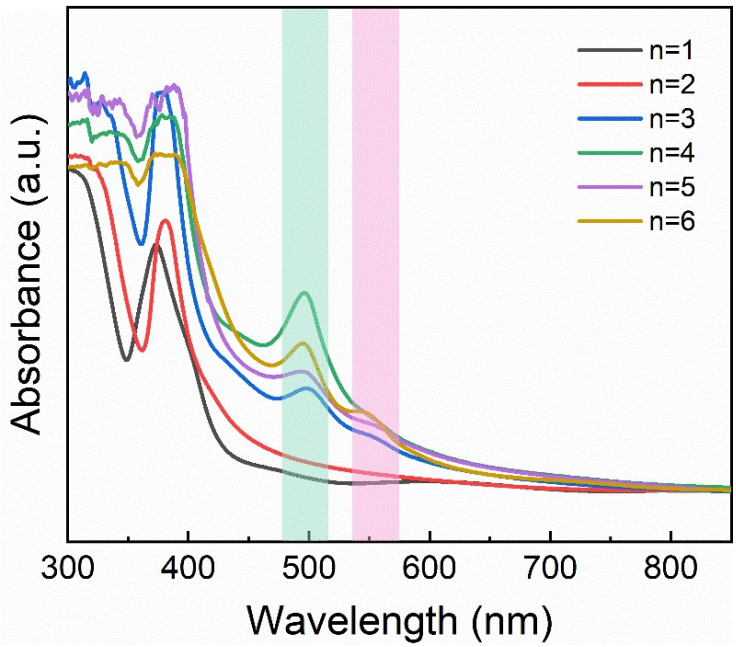

Fig. S6 UV-vis absorption spectrum of different n-value $DMA_2FA_{n-1}Pb_nI_{3n+1}$ film. Two peaks located at ~500 nm and ~550 nm appeared when n is greater than 2, respectively, indicating that DMAI post treatment in this work actually formed 2D perovskite with mixed phase.

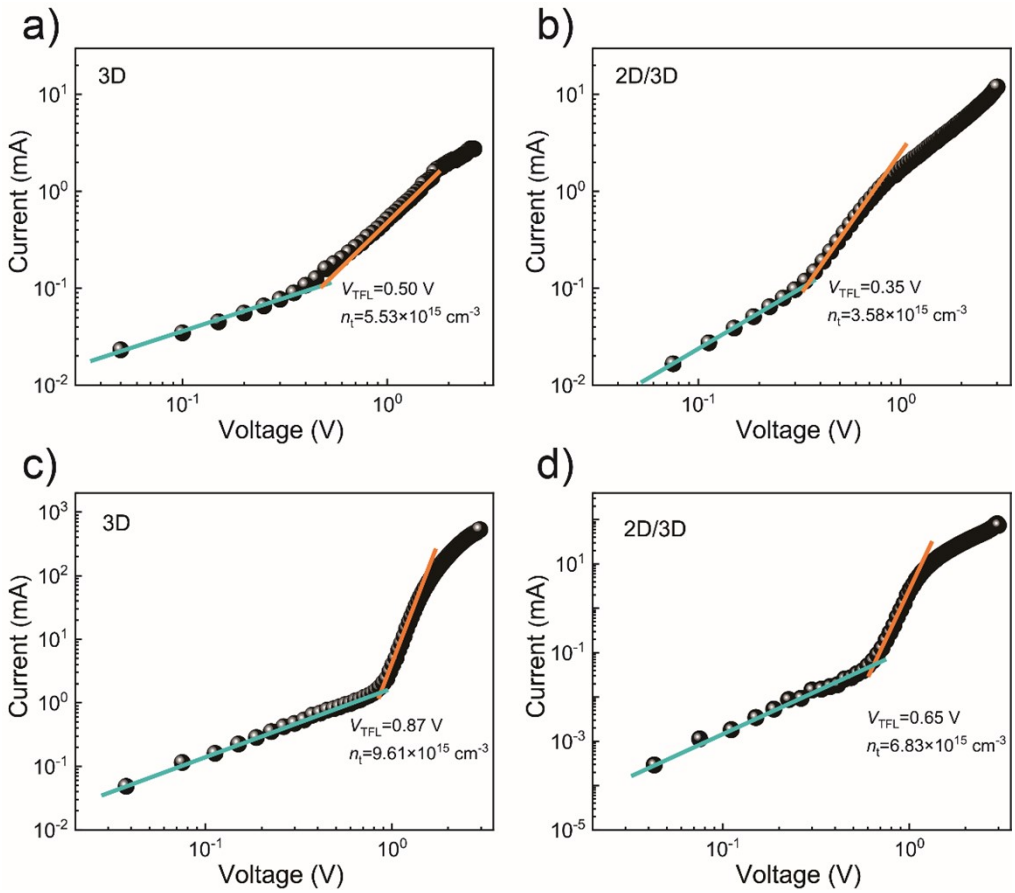

Fig. S7 Space charge limited current (SCLC) measurements of electron-only devices based on a) 3D perovskite film and b)2D/3D perovskite film; hole-only devices based on c) 3D perovskite film and d) 2D/3D perovskite film.

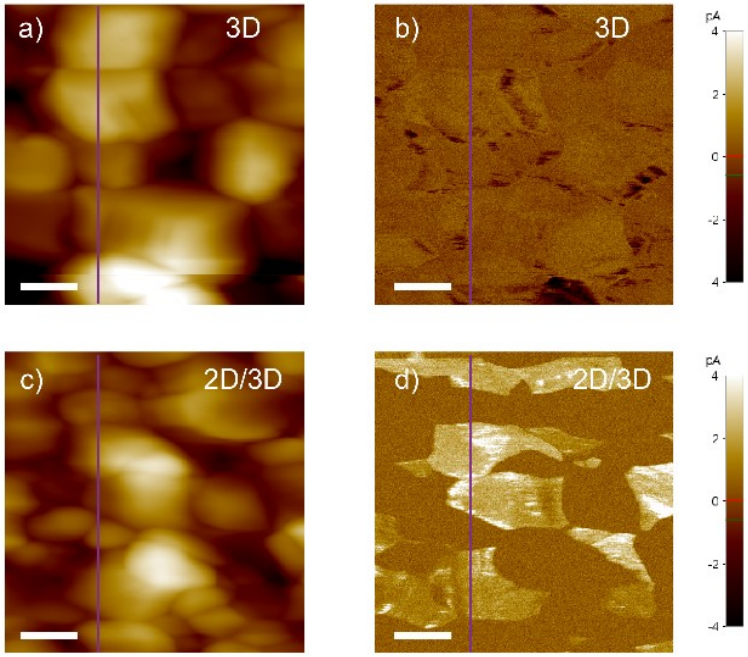

Fig. S8 Topographic morphology image of a) 3D perovskite film, C) 2D/3D perovskite film and current mapping image of b) 3D perovskite film, d) 2D/3D perovskite film which are deposited on FTO substrates. The scale bar is 200 nm.

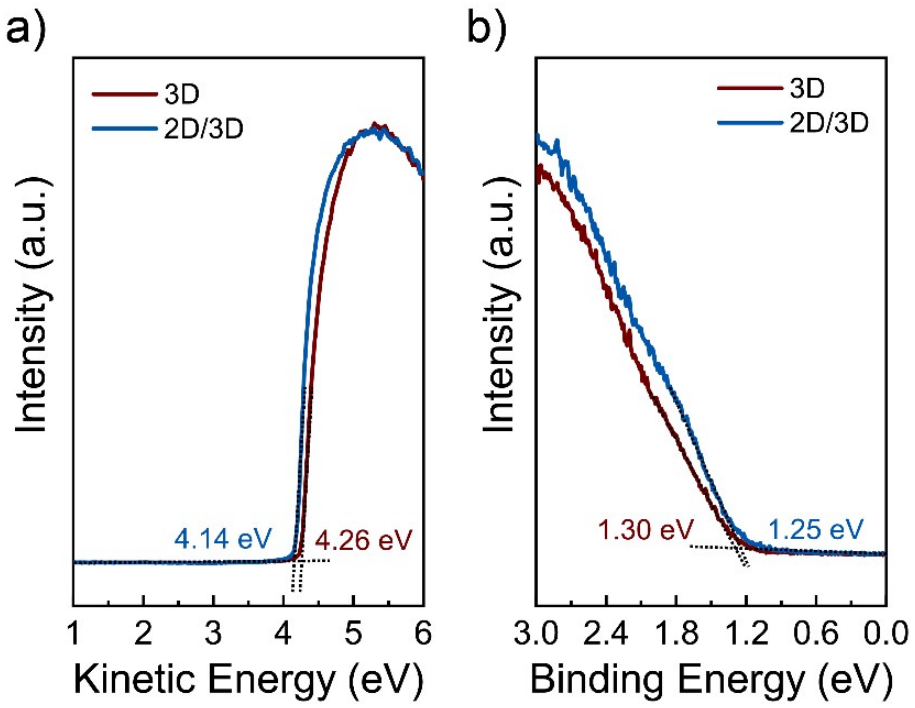

Fig. S9 UPS spectra of 3D perovskite film and 2D/3D perovskite film a) the secondary electron cut-off region and b) the magnified spectra near Fermi edge.

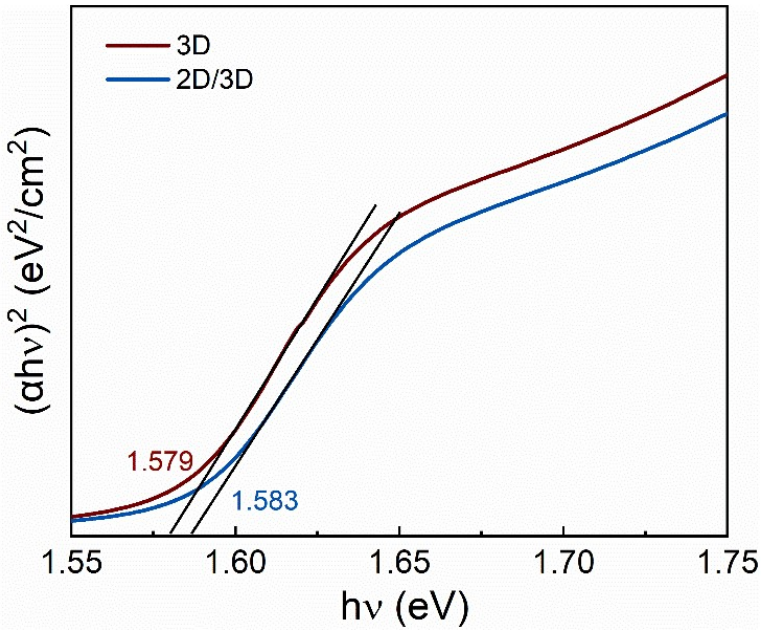

Fig. S10 Tauc plots of absorbance with photon energy (hν) and extracted bandgap of 3D perovskite and 2D/3D perovskite film.

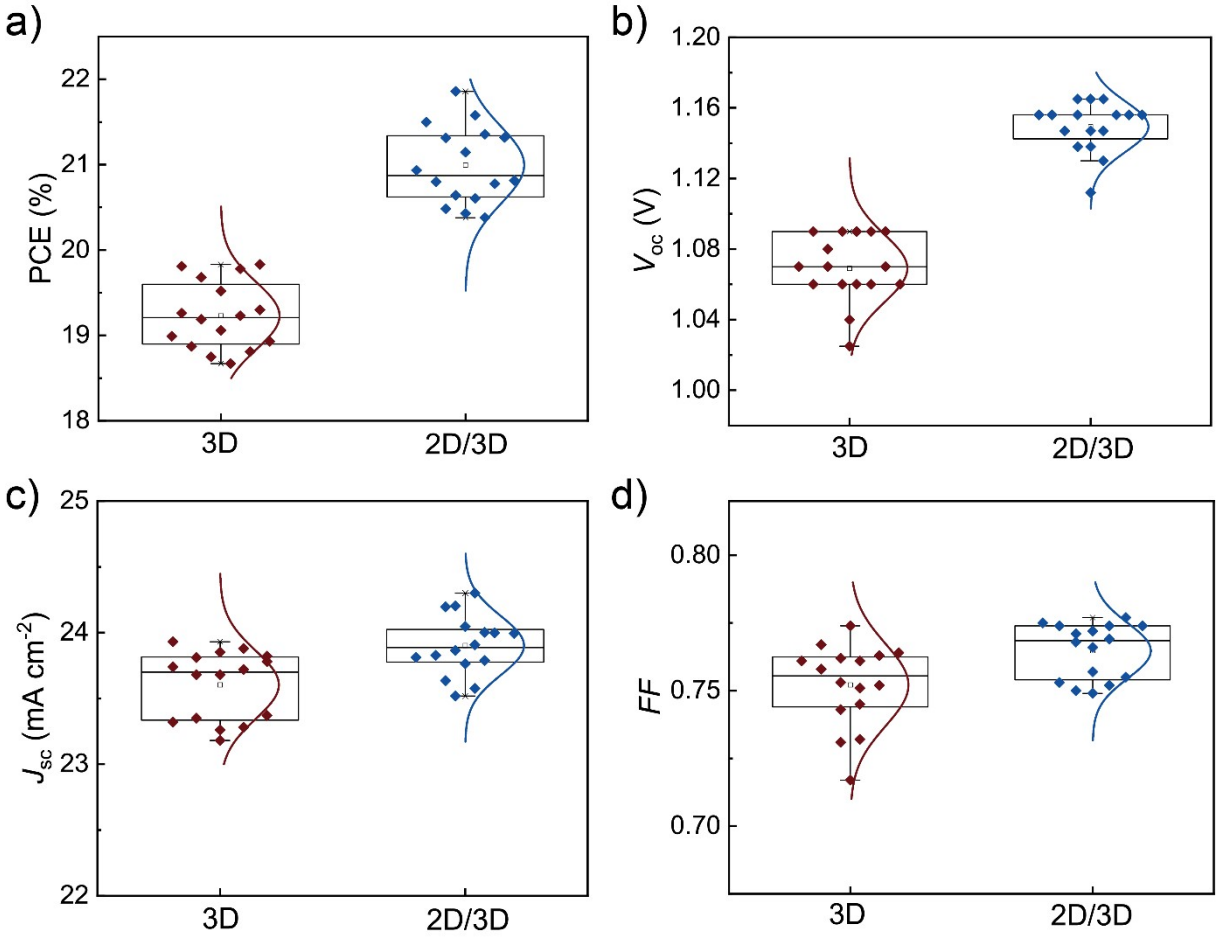

Fig. S11 Statistical distribution of the a) PCE, b) V_{OC}, c) J_{sc} and d) *FF* of the PSCs based on 3D perovskite and 3D perovskite. The data were collected among 16 cells and all cells were measured at the reverse scan.

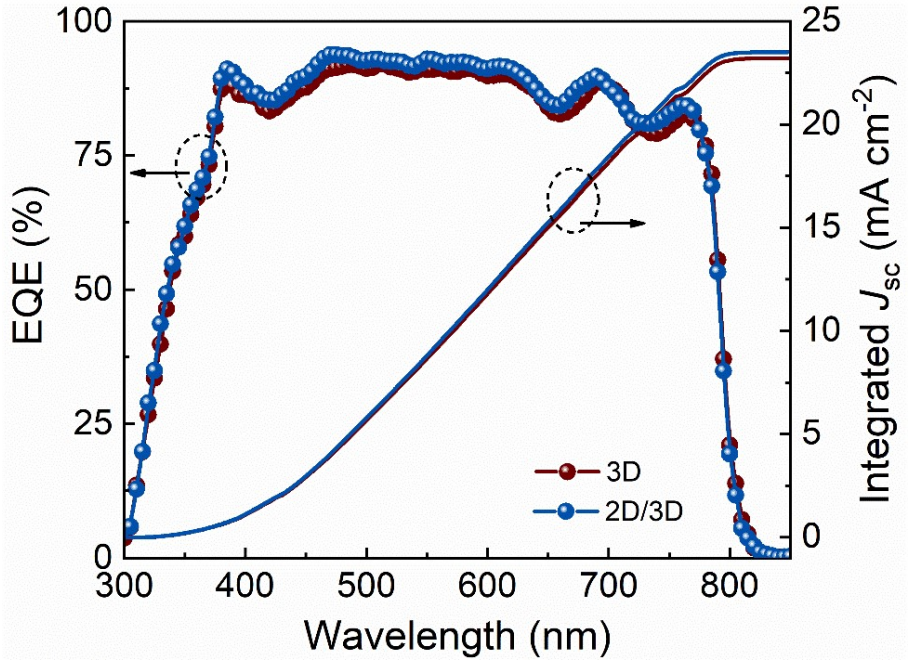

Fig. S12 External quantum efficiency (EQE) spectrum of devices based on 3D perovskite and 2D/3D perovskite.

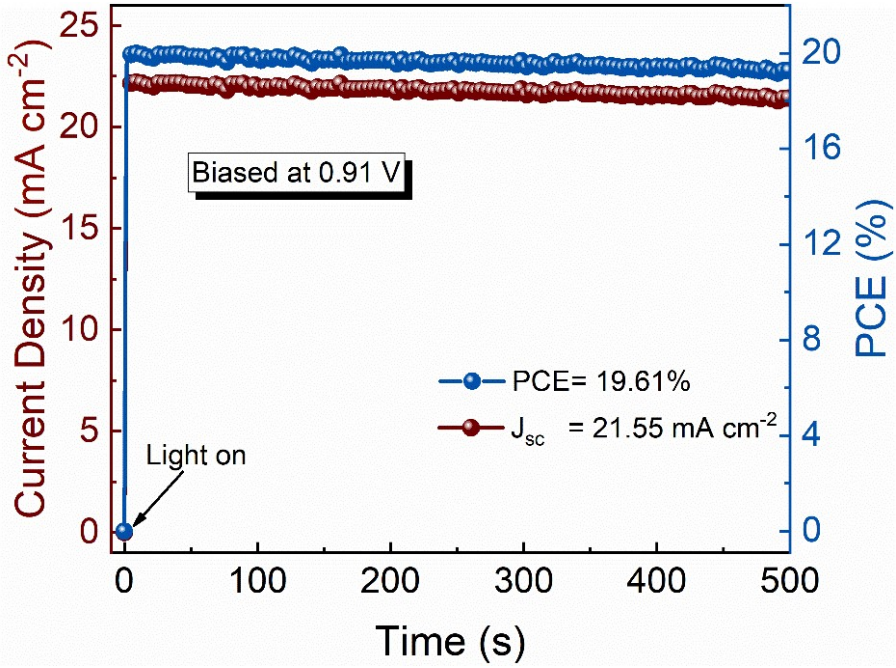

Fig. S13 Stabilized current density (*J*) and PCE at the maximum power point (0.91 V) of the control devices based on 3D perovskite.

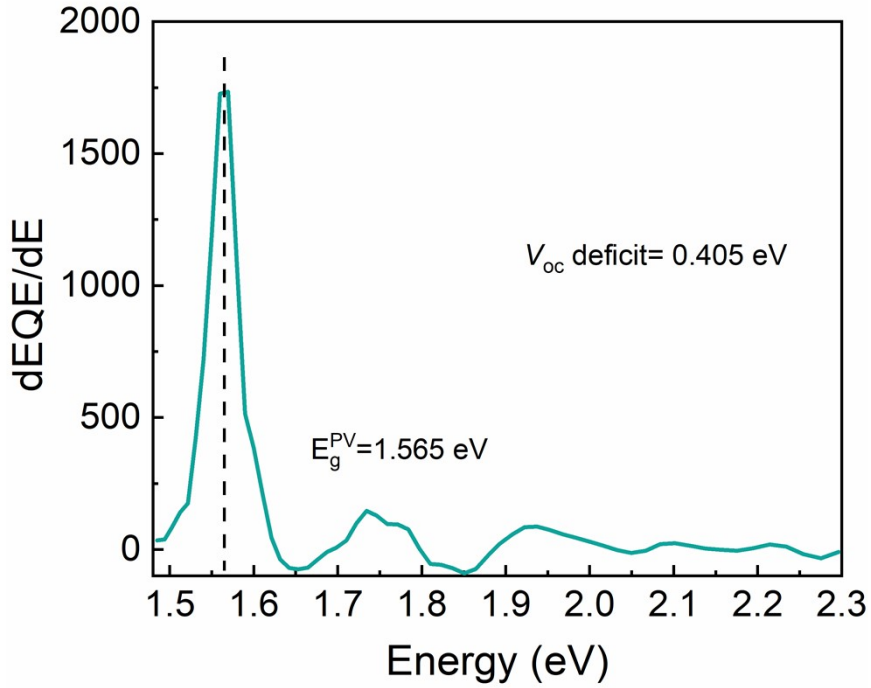

Fig. S14 The photovoltaic bandgap for Voc deficit calculation is obtained from maximum point of the derivative of the EQE spectra (dEQE/dE).

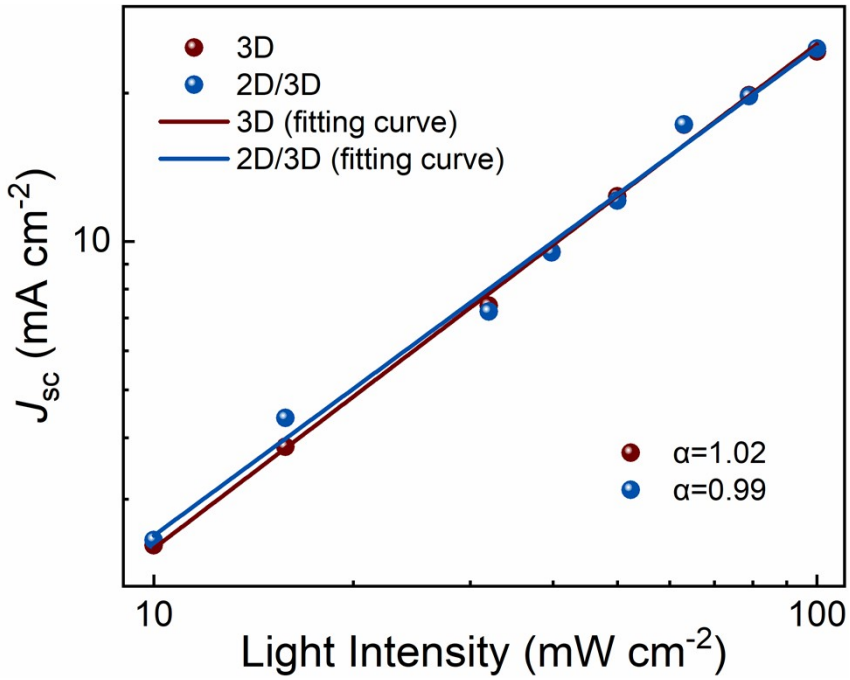

Fig. S15 The light intensity dependence of J_{sc} of devices based on 3D perovskite and 2D/3D perovskite.

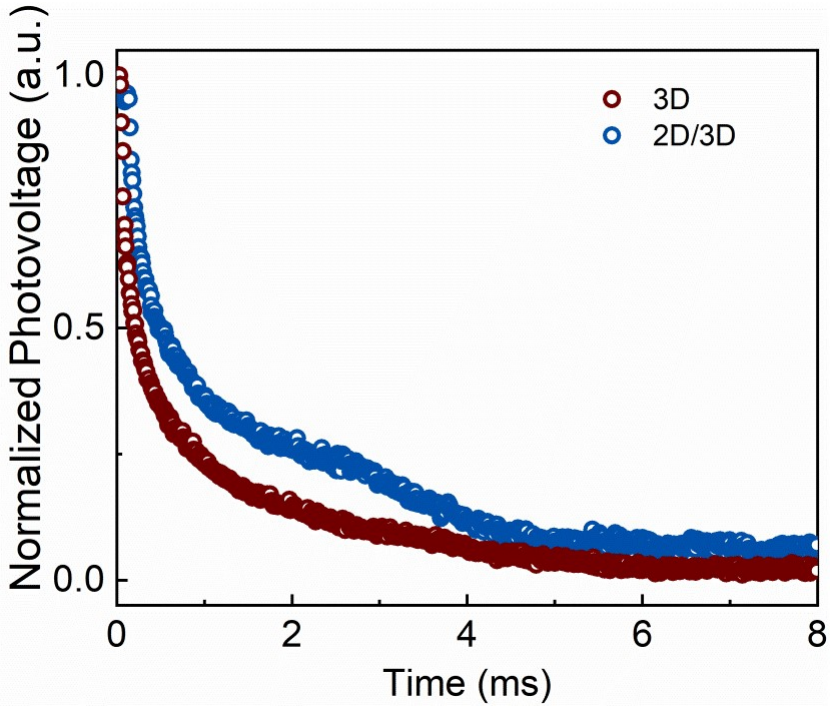

Fig. S16 Transient photovoltage (TPV) decay spectroscopy of the devices based on 3D perovskite and 2D/3D perovskite.

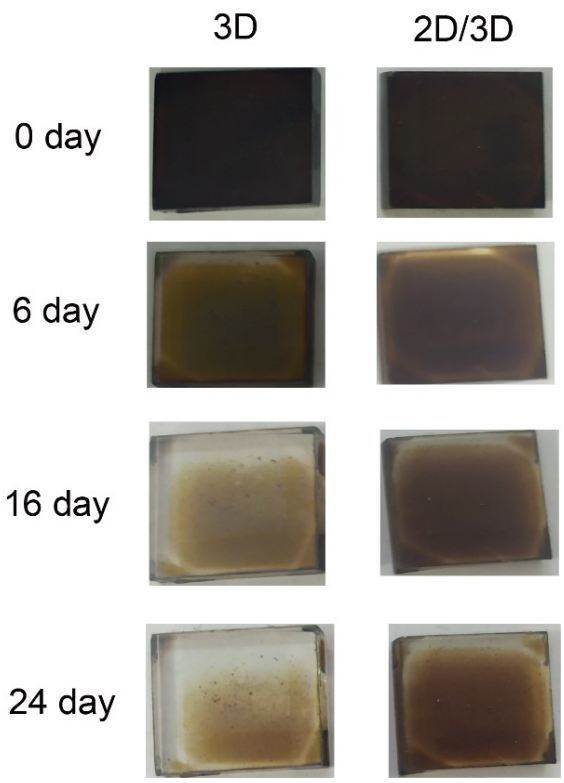

Fig. S17 The photographs of the 3D and 2D/3D perovskite films on FTO/Glass exposed to the air environment with the relative humidity of 50%.

Table S1. Fitting parameters of decay amplitude and decay time obtained from TRPL spectra.

	A_1	τ_1 (ns)	A_2	τ_2 (ns)	τ_{avg} (ns)
3D	18.00	17.81	82.00	238.05	232.09
2D/3D	15.43	19.32	84.57	347.41	347.42

Table S2. PV device parameters of the PSCs with different concentrations of DMAI, measured under the reverse scan.

Concentration	V_{oc} (V)	J_{sc} (mA cm^{-2})	*FF*	PCE (%)
0 mg mL^{-1}	1.09	23.82	0.76	19.83
1 mg mL^{-1}	1.11	24.04	0.77	20.54
3 mg mL^{-1}	1.16	24.20	0.78	21.90
5 mg mL^{-1}	1.14	23.32	0.76	20.20
7 mg mL^{-1}	1.11	22.45	0.75	18.88

Table S3. PV device parameters of the PSCs with different annealing temperature of DMAI treatment, measured under the reverse scan.

Temperature	V_{oc} (V)	J_{sc} (mA cm^{-2})	*FF*	PCE (%)
Control	23.74	1.07	0.75	19.30
No annealing	23.51	1.12	0.76	20.18
80 ^{o}C	23.76	1.14	0.75	20.43
100 ^{o}C	23.99	1.15	0.78	21.57
120 ^{o}C	23.64	1.10	0.77	20.04
140 ^{o}C	23.85	1.09	0.71	18.75

Table S4. PV device parameters of the PSCs with different annealing time of DMAI treatment, measured under the reverse scan.

Time	V_{oc} (V)	J_{sc} (mA cm^{-2})	*FF*	PCE (%)
Control	23.88	1.07	0.77	19.78
3 min	24.04	1.11	0.77	20.64
5 min	24.00	1.15	0.78	21.49
7 min	23.72	1.08	0.74	19.19

Table S5. PV device parameters extracted from *J-V* scans of devices based on 3D perovskite and 2D/3D perovskite.

Condition	Scan direction	V_{oc} (V)	J_{sc} (mA cm^{-2})	*FF*	PCE (%)	*H*-index
3D	reverse	1.09	23.82	0.76	19.83	0.039
	forward	1.06	23.65	0.76	19.05	
	average [a)]	1.07±0.02	23.60±0.26	0.75±0.01	19.23±0.39	
2D/3D	reverse	1.16	24.20	0.78	21.90	0.021
	forward	1.16	24.00	0.77	21.43	
	average	1.15±0.01	23.86±0.29	0.76±0.01	21.00±0.45	

a) The data were collected among 16 cells and the cells were measured under the reverse scan.

Table S6. EIS parameters of devices based on 3D perovskite and 2D/3D perovskite.

	R_s (Ohm)	R_{rec} (Ohm)	C_{rec} (F)
3D	49.22	74.68	8.91×10^{-9}
2D/3D	22.31	352.70	1.07×10^{-8}